A&A 452, 487–492 (2006)
DOI: 10.1051/0004-6361:20054026

Astronomy & Astrophysics

Star formation in molecular cores

III. The effect of the turbulent power spectrum

S. P. Goodwin, A. P. Whitworth, and D. Ward-Thompson

Dept. of Physics & Astronomy, Cardiff University, 5 The Parade, Cardiff, CF24 3YB, Wales, UK
e-mail: Simon.Goodwin@astro.cf.ac.uk

Received 10 August 2005 / Accepted 2 February 2006

ABSTRACT

We investigate the effect of the turbulent power spectrum ($P(k) \propto k^{-n}$, with $n = 3$, 4 or 5) on the fragmentation of low-mass cores, by means of SPH simulations. We adopt initial density profiles and low levels of turbulence based on observation, and for each n-value we conduct an ensemble of simulations with different initial seeds for the turbulent velocity field, so as to obtain reasonable statistics. We find that when power is concentrated at larger scales (i.e. for larger n), more protostellar objects form and there is a higher proportion of low-mass stars and brown dwarfs. This is in direct contrast with the recent results of Delgado Donate et al., presumably because they adopted much higher levels of turbulence.

Key words. stars: formation

1. Introduction

Stars form in dense molecular cores (e.g. André et al. 2000), and most stars – especially young stars – are in multiple systems (e.g. Duquennoy & Mayor 1991; Mathieu 1994; Duchêne 1999; Patience et al. 2002), which implies that star-forming cores usually fragment into multiple objects.

Simulations suggest that cores are prone to fragment into multiple objects under a variety of circumstances: (i) if they possess a small amount of initial rotation (e.g. Burkert & Bodenheimer 1996); (ii) if their collapse is triggered by a sudden increase in external pressure (e.g. Hennebelle et al. 2003, 2004); or (iii) if they contain turbulence. The level of turbulence can be high (e.g. Bate et al. 2002, 2003; Delgado Donate et al. 2004) or low (e.g. Goodwin et al. 2004a,b).

This is the third in a series of papers investigating the collapse and fragmentation of cores with initial density profiles and levels of turbulence based on observation. In Paper I (Goodwin et al. 2004a) we have shown that cores with even a very low level of turbulence can fragment into multiple objects, but the number of fragments that form is very sensitive to the details of the initial turbulent velocity field. In Paper II (Goodwin et al. 2004b) we have shown that the number of fragments increases as the level of turbulence is increased. In this paper we investigate the effect of the power spectrum of turbulence on the fragmentation of cores with *low* levels of turbulence. A similar investigation has already been made by Delgado Donate et al. (2004) for cores with *high* levels of turbulence, and there are significant differences between their results and ours, which we explain in Sect. 4.

In Sect. 2 we describe the initial conditions and numerical methods used. In Sect. 3 we present our results, in Sect. 4 we discuss them, and in Sect. 5 we summarise our main conclusions.

2. Initial conditions and numerical method

The density profiles of prestellar cores are approximately flat in the centre, and then decrease as $r^{-\nu}$ with $2 \leq \nu \leq 5$ in their outer parts, until they merge with the background (e.g. Ward-Thompson et al. 1994, 1999; André et al. 1996, 2000; Tafalla et al. 2004; Kirk et al. 2005). A good fit to the density profile is given by

$$\rho(r) = \frac{\rho_{\rm kernel}}{(1 + (r/R_{\rm kernel})^2)^2}, \tag{1}$$

where $\rho_{\rm kernel}$ is the central density and $R_{\rm kernel}$ is the radius of the region in which the density is approximately uniform (cf. Whitworth & Ward-Thompson 2001). We set $\rho_{\rm kernel} = 3 \times 10^{-18}\,{\rm g\,cm^{-3}}$ and $R_{\rm kernel} = 5000\,{\rm AU}$, with the outer boundary of the core at $R_{\rm core} = 50\,000\,{\rm AU}$, so the total mass of the core is $M_{\rm core} = 5.4\,M_\odot$. These parameters are typical of low-mass star forming cores (e.g. Jijina et al. 1999). The core is initially isothermal, with $T = 10\,{\rm K}$, and molecular, with mean gas-particle mass $\bar{m} = 4 \times 10^{-24}\,{\rm g}$. Hence the core has a ratio of thermal to gravitational energy of

$$\alpha_{\rm therm} \equiv \frac{U_{\rm therm}}{|\Omega|} \simeq 0.3. \tag{2}$$

The line widths of molecular cores show a significant non-thermal contribution (e.g. Myers 1983, 1991; Jijina et al. 1999), which is attributable to internal turbulence. Figure 1 shows the estimated ratios of turbulent to gravitational energy,

$$\alpha_{\rm turb} \equiv \frac{U_{\rm turb}}{|\Omega|}, \tag{3}$$

and the estimated masses, $M_{\rm core}$, for prestellar cores from the Jijina et al. (1999) catalogue. These cores have been selected as prestellar on the basis of having low temperature (<20 K), no associated IRAS source and no observed outflow. Using Fig. 1

Table 1. For each value of n, we list the number of realisations simulated ($\mathcal{N}_{\rm real}$); the mean mass in objects at the end of a simulation ($M_{\rm tot}/M_\odot$); the mean number of objects formed per simulation $\left(\bar{\mathcal{N}}_{\rm obj}\right)$ and its variance; the mean number of stars ejected from a core ($\mathcal{N}_{\rm ej}$); the net ratio of brown dwarfs to stars ($\mathcal{N}_{\rm BD}/\mathcal{N}_*$); the fraction of all objects that are single ($S/\mathcal{N}_{\rm obj}$); the median semi-major axis ($a_{\rm med}$); the mean mass-ratio for binary systems ($\bar{q}$); the variance of the mass ratio of binary systems (σ_q); and the mean numbers of singles ($\bar{S}$), binaries ($\bar{B}$), triples ($\bar{T}$), quadruples ($\bar{Q}$), and quintuples ($\bar{Q}'$) formed by one core.

n	$\mathcal{N}_{\rm real}$	$M_{\rm tot}/M_\odot$	$\bar{\mathcal{N}}_{\rm obj}$	$\mathcal{N}_{\rm ej}$	$\mathcal{N}_{\rm BD}/\mathcal{N}_*$	$S/\mathcal{N}_{\rm obj}$	$a_{\rm med}$	$\bar{q}$	σ_q	$\bar{S}$	$\bar{B}$	$\bar{T}$	$\bar{Q}$	$\bar{Q}'$
3	10	3.39	3.7 ± 1.4	0.80	0.08	0.22	13	0.74	0.17	0.80	0.20	0.30	0.40	0
4	20	3.35	4.8 ± 3.1	1.95	0.20	0.41	9	0.83	0.26	1.95	0.25	0.35	0.25	0.05
5	10	3.41	5.5 ± 3.0	2.10	0.15	0.38	6	0.65	0.21	2.10	0.20	0.40	0.20	0.20

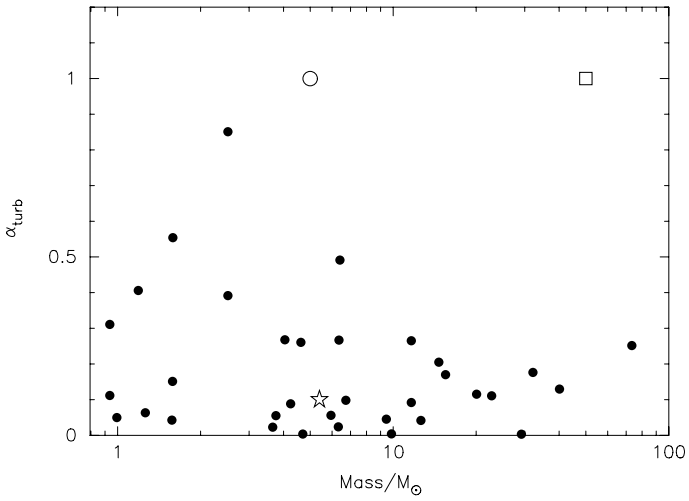

Fig. 1. The filled circles give estimated values of $\alpha_{\rm turb}$ (the ratio of turbulent to gravitational energy) and $M_{\rm core}$ (core mass) for the starless cores in the Jijina et al. (1999) catalogue. The open star shows the values used in this paper: $\alpha_{\rm turb} = 0.1$ and $M_{\rm core} = 5.4\ M_\odot$. The open circle shows the values used by Delgado Donate et al. (2004): $\alpha_{\rm turb} = 1.0$ and $M_{\rm core} = 5.0\ M_\odot$. The open square shows the values used by Bate et al. (2002, 2003): $\alpha_{\rm turb} = 1.0$ and $M_{\rm core} = 50\ M_\odot$. Some of the cores in the Jijina et al. catalogue have already started to collapse, and therefore systematic infall motions are making a contribution to their non-thermal line-widths, thus causing us to over-estimate their $\alpha_{\rm turb}$. Hence, we believe that our choice of $\alpha_{\rm turb}$ is more representative of the initial conditions in these cores.

as a guide, we adopt $\alpha_{\rm turb} = 0.1$, and hence a total virial ratio of $\alpha_{\rm turb} + \alpha_{\rm therm} \sim 0.4$, for all the simulations in this paper.

To model the turbulence in a core, we impose a divergence-free gaussian random velocity field with power spectrum $P(k) \propto k^{-n}$ (cf. Bate et al. 2002, 2003; Fisher 2004; Bonnell et al. 2003; Delgado-Donate et al. 2003, 2004). The observed velocity fields in GMCs and cores are well represented by turbulent power spectra of this form with $n = 3$ to 4 (Burkert & Bodenheimer 2000).

In this paper we present two ensembles of 10 simulations each, one with $n = 3$ and one with $n = 5$, and compare these with the ensemble of 20 simulations with $n = 4$ already presented in Paper II. Within an ensemble, each simulation differs only in the random seed used to initialise the turbulent velocity field.

2.1. Computation method and constitutive physics

The simulations are performed with the DRAGON code (Goodwin et al. 2004a), which is based on a standard implementation of SPH (e.g. Monaghan 1992). An octal tree (Barnes & Hut 1984) is used to evaluate gravitational accelerations and to identify SPH neighbours. Particle smoothing lengths are adjusted so that each particle has $N_{\rm neib} = 50 \pm 5$ neighbours. Gravity is kernel softened with the particle smoothing lengths, and standard artificial viscosity is included with $\alpha_v = 1$ and $\beta_v = 2$. The interested reader is referred to Paper I for further details.

At low densities, radiative cooling is efficient and the gas in a core is approximately isothermal at $T_0 \sim 10\,{\rm K}$. However, once the density exceeds $\rho_{\rm crit} \sim 10^{-13}\,{\rm g\,cm^{-3}}$, the optical depth through a core becomes too large for efficient cooling (Larson 1969; Tohline 1982; Masunaga & Inutsuka 2000) and the gas switches to being approximately adiabatic. We model this behaviour with a barotropic equation of state (e.g. Tohline 1982; Masunaga & Inutsuka 2000):

$$\frac{P}{\rho} = c_0^2 \left[1 + \left(\frac{\rho}{\rho_{\rm crit}} \right)^{2/3} \right]. \tag{4}$$

Here P is the pressure, ρ is the density, and $c_0 \approx 0.19\,{\rm km\,s^{-1}}$ is the isothermal sound speed in molecular gas at $T \simeq 10\,{\rm K}$.

Following the evolution of dense regions that are collapsing to stellar densities is very expensive computationally. In order to avoid this expense, wherever a bound regions forms with $\rho > 100\,\rho_{\rm crit}$ we replace it with a sink particle (Bate et al. 1995). A sink particle interacts with the gas gravitationally, and it accretes any SPH particle which (a) approaches closer than 10 AU and (b) is bound to it. When an SPH particle is accreted by a sink particle, the sink particle acquires the mass, linear momentum and angular momentum of the SPH particle, and therefore we can still monitor the conservation of these quantities as a check on the fidelity of the code. We refer to sink particles generically as "objects"; and then, more specifically, as "stars" when the sink mass is greater than $0.08\ M_\odot$, and as "brown dwarfs" when the mass is lower than this.

3. Results

We have performed two ensembles of 10 simulations each, one ensemble using $P(k) \propto k^{-3}$ and one ensemble using $P(k) \propto k^{-5}$. These are then compared with the ensemble of 20 simulations using $P(k) \propto k^{-4}$ reported in Paper II. All simulations treat cores with $\alpha_{\rm turb} = 0.10$. A summary of the results is given in Table 1. The details of each simulation are presented in Table 2.

3.1. The number of objects formed

The fragmentation of a collapsing, mildly turbulent core usually starts with the formation of a primary protostar surrounded by a rotating, but very unrelaxed, disc. The inflow of material onto the disc is very inhomogeneous and irregular, and as it joins the disc it causes spiral arms to develop. If these arms become sufficiently dense, they fragment to form secondary companions (e.g. Goodwin et al. 2004a,b; Gawryszczak et al. 2006). If n is low, most of the turbulent energy is concentrated on small scales, but

Table 2. The results of the individual simulations; in all cases $\alpha_{\rm turb} = 0.10$. Column 1 gives the simulation identifier and Col. 2 gives n (the exponent of the turbulent power spectrum, $P(k) \propto k^{-n}$). Column 3 gives $M_{\rm obj}$ (the total mass of objects formed, stars plus brown dwarfs), Col. 4 gives $N_{\rm obj}$ (the total number of objects formed) and Col. 5 gives $N_{\rm bd}$ (the total number of brown dwarfs formed). Column 6 gives the multiplicities of the multiple systems formed, and Col. 7 gives the mass of each individual object. Those objects which are part of a binary system are distinguished with ^{b}, those which are part of a triple system with ^{t}, and those which are part of a quadruple or quintuple system with ^{q}. Two realisations have ejected binary systems.

ID	n	$M_{\rm obj}$	$N_{\rm obj}$	$N_{\rm bd}$	Multiplicity	Masses/$M_\odot$
571	3	3.04	4	0	Triple	1.06^t, 0.77^t, 0.61, 0.59^t
572	3	3.21	5	0	Quadruple	1.24^q, 0.75^q, 0.60^q, 0.47, 0.14^q
573	3	3.62	5	1	Quadruple	1.43^q, 0.78^q, 0.75^q, 0.62^q, 0.04
574	3	3.20	5	0	Triple	0.89^t, 0.80^t, 0.80^t, 0.57, 0.14
575	3	2.95	1	0	Single	2.95
576	3	3.79	5	1	Quadruple	1.05^q, 1.05^q, 0.86^q, 0.74^q, 0.09
577	3	3.58	2	0	Binary	2.01^b, 1.57^b
578	3	2.97	4	1	Triple	2.04^t, 0.45^t, 0.45^t, 0.02
579	3	3.79	2	0	Binary	2.47^b, 1.33^b
580	3	3.76	4	0	Quadruple	1.36^q, 0.81^q, 0.80^q, 0.79^q
001	4	3.78	3	0	Triple	1.49^t, 1.15^t, 1.13^t
002	4	2.83	1	0	Single	2.38
003	4	3.72	1	0	Single	3.72
004	4	3.48	1	0	Single	3.48
005	4	2.86	4	1	Binary	1.43^b, 0.77, 0.65^b, 0.02
006	4	2.84	1	0	Single	2.84
007	4	3.15	5	0	Triple & Binary	1.76^t, 0.72^t, 0.47^t, 0.10^b, 0.10^b
008	4	3.22	6	2	Quadruple	1.97^q, 0.47^q, 0.35^q, 0.34^q, 0.06, 0.03
009	4	3.48	8	4	Quadruple	2.28^q, 0.49^q, 0.26^q, 0.25^q, 0.08, 0.05, 0.04, 0.04
010	4	3.31	8	1	Quadruple	0.76^q, 0.74^q, 0.58^q, 0.57^q, 0.46, 0.09, 0.08, 0.03
011	4	3.96	12	4	Triple & binary?	0.89^t, 0.82^t, 0.82^t, 0.42, 0.38, 0.25, 0.12, 0.11, 0.04^b, 0.04^b, 0.03, 0.03
012	4	3.60	6	2	Triple	1.34^t, 0.92^t, 0.79^t, 0.50, 0.04, 0.02
013	4	3.18	10	3	Quadruple & binary	0.77^q, 0.68^q, 0.61^q, 0.60^q, 0.11^b, 0.11^b, 0.10, 0.06, 0.05, 0.04
014	4	3.29	4	1	Binary	1.58^b, 1.16^b, 0.49, 0.08
015	4	2.48	1	0	Single	2.48
016	4	3.58	4	0	Triple	1.23^t, 1.15^t, 1.11^t, 0.09
017	4	3.41	8	0	Quintuple	1.10^q, 0.98^q, 0.32^q, 0.27^q, 0.27^q, 0.17, 0.15, 0.14
018	4	3.48	4	0	Quadruple	0.98^q, 0.94^q, 0.79^q, 0.77^q
019	4	3.58	5	1	Triple	1.38^t, 1.03^t, 1.00^t, 0.11, 0.06
020	4	3.77	3	0	Triple	1.28^t, 1.27^t, 1.22^t
551	5	3.21	1	0	Single	3.21
552	5	3.34	7	0	Quadruple	0.69^q, 0.59^q, 0.57^q, 0.52^q, 0.45, 0.37, 0.15
553	5	3.46	6	0	Triple	1.29^t, 1.11^t, 0.49, 0.29^t, 0.17, 0.10
554	5	3.22	8	2	Quadruple	1.10^q, 0.75^q, 0.71^q, 0.27^q, 0.18, 0.15, 0.04, 0.01
555	5	3.52	5	0	Quintuple	1.16^q, 0.84^q, 0.60^q, 0.51^q, 0.40^q
556	5	3.39	1	0	Single	3.39
557	5	3.77	7	1	Triple + Binary	1.45^t, 0.93^t, 0.89^t, 0.22^b, 0.13^b, 0.13, 0.01
558	5	3.10	11	3	Quintuple + Binary	0.83^q, 0.57^q, 0.43^q, 0.35^q, 0.30^q, 0.29, 0.14, 0.09, 0.04, 0.02^b, 0.02^b
559	5	3.75	6	2	Triple	1.13^t, 0.97^t, 0.80^t, 0.79, 0.03, 0.03
560	5	3.30	3	0	Triple	2.25^t, 0.59^t, 0.46^t

the resulting inhomogeneities in the inflow are of such low amplitude that the spiral perturbations they seed in the disc tend to be dissipated by the shear in the disc rather than being amplified by self-gravity. Conversely, if n is large, most of the turbulent energy is concentrated on large scales, and although the resulting inhomogeneities are again of low amplitude, they are of sufficiently large mass that the spiral perturbations they seed in the disc have a better chance of being amplified by self-gravity and fragmenting into secondary companions. As n is increased from $n = 3$ to $n = 5$, more power is invested in large-scale turbulence, and therefore there tend to be more objects formed. When $n = 3$, $\bar{N}_{\rm obj} = 3.7 \pm 1.4$; but when $n = 5$, this increases to $\bar{N}_{\rm obj} = 5.5 \pm 3.0$.

We stress that the large variance on $\bar{N}_{\rm obj}$ is because this is a chaotic process, and two simulations from the same ensemble (same $\alpha_{\rm turb}$ and n) can produce two vastly different sets of objects. For example one simulation from the ensemble with $n = 4$ produces a quadruple, a binary and four singles, whilst several others produce just one star (see Table 2). Nonetheless, a generic trend is seen.

3.2. Mass functions and companion probabilities

Once an object forms, its final mass is determined by competitive accretion (Bonnell et al. 2001) and dynamical interaction with other objects. Competitive accretion causes the more massive objects, and/or those which reside in the dense material at the centre of the core, to grow rapidly in mass. Dynamical interaction causes some objects, usually the lower-mass ones, to be ejected from the dense material at the centre of the core, so that the remaining objects become more tightly bound and some eventually end up in stable multiple systems. Thus, in general, it is the lower-mass objects (low-mass stars and brown dwarfs) which are ejected as singles before they can accrete much mass

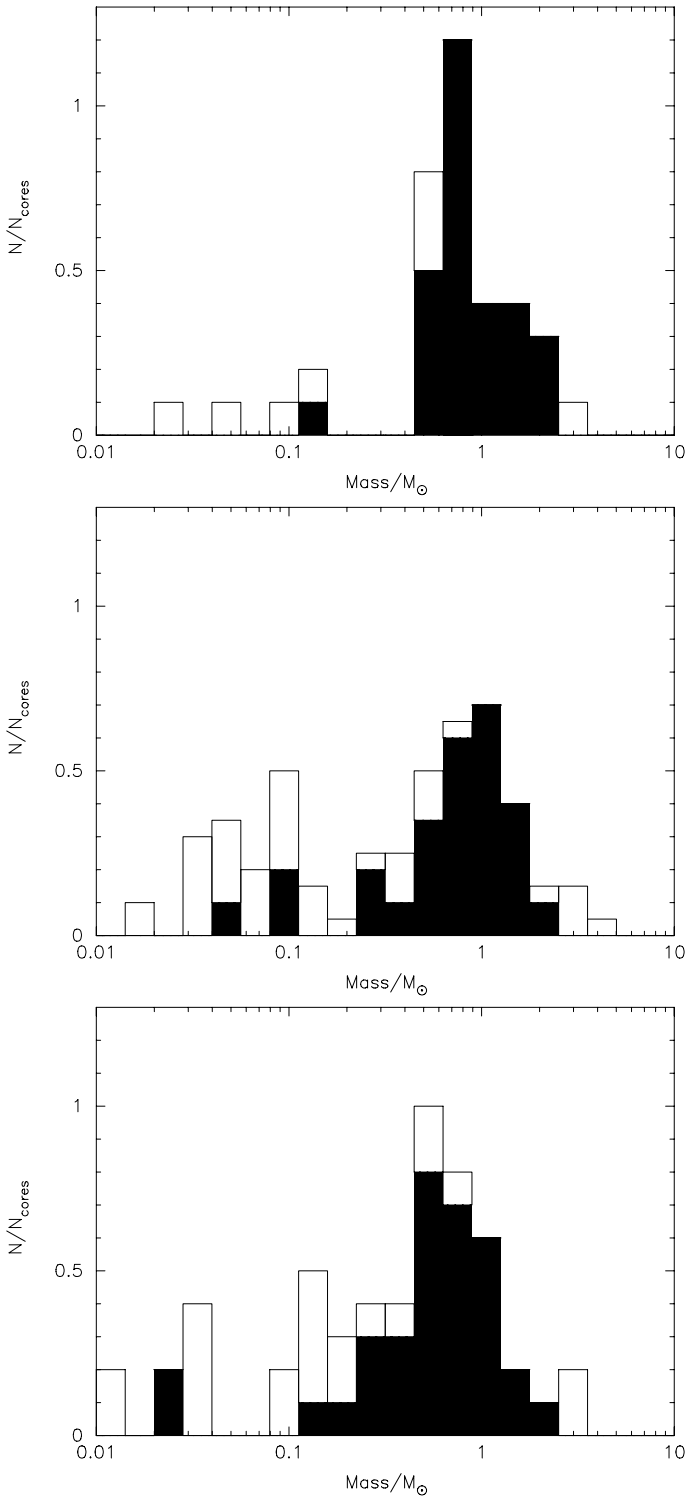

Fig. 2. Normalised mass functions for objects spawned by cores with $n = 3$ (*top*), $n = 4$ (*middle*) and $n = 5$ (*bottom*). The filled portion of each histogram represents objects in multiple systems, while the open portion represents single objects.

(Reipurth & Clarke 2001); and the higher-mass objects ($\sim 1\,M_\odot$) which remain in the centre of the core, and form multiples.

Figure 2 shows the mass functions from the three ensembles with $n = 3$ (top), $n = 4$ (middle) and $n = 5$ (bottom). In each case the filled portion of the histogram represents objects in multiple systems, and the open portion represents single objects.

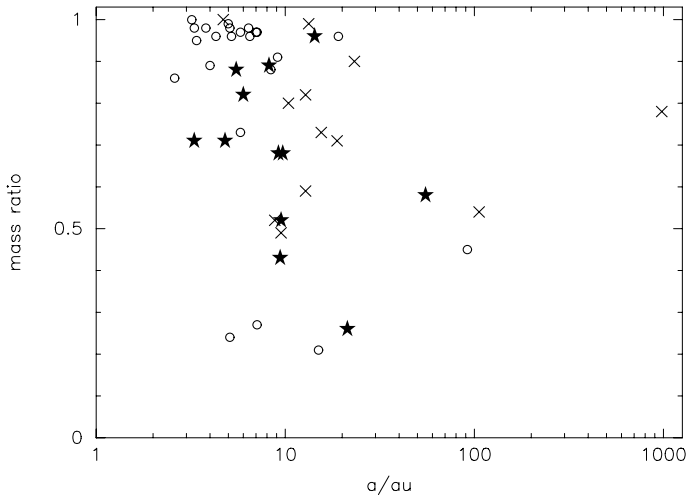

Fig. 3. Mass ratio, q, against separation, a, for binaries spawned by cores with $n = 3$ (crosses), $n = 4$ (open circles) and $n = 5$ (solid stars).

The mass functions for $n = 4$ and $n = 5$ are very similar. There is a broad peak around 1 $M_\odot$, consisting mainly of objects in multiple systems, and a flat tail of lower-mass objects consisting mainly of ejected singles. Because of the large number of ejected singles, the overall companion probability is low, ~0.6.

In contrast, when $n = 3$, the mass function is dominated by the peak around $\sim 1\,M_\odot$ and there are very few ejected singles. This is because, when $n = 3$, an individual core spawns fewer objects, and therefore fewer ejections are required to stabilise the remaining multiple system. The paucity of ejected singles gives a much higher overall companion probability, ~0.8.

3.3. Binary separations and mass ratios

In all cases ($n = 3$, 4 and 5), the distribution of separations is much narrower than that observed by Duquennoy & Mayor for local G dwarfs, which is not surprising, since we have considered only one core mass, and only one level of turbulence[1]. In particular there is a total lack of wide binaries ($a > 100$ AU). For $n = 3$, most binaries have separations in the range 10 to 30 AU, and there is only one hard binary ($a < 10$ AU). In contrast, when $n = 4$, 17 of the 20 binaries formed have $a < 10$ AU; and when $n = 5$, 10 of the 13 binaries formed have $a < 10$ AU. This difference arises because a core with larger n tends to spawn more objects, and so on average more ejections are needed before a stable multiple is left; specifically, the average number of objects ejected from a core is only 0.80 for $n = 3$, but 1.95 for $n = 4$ and 2.10 for $n = 5$. Since each ejection hardens the multiple that is left behind, the greater number of ejections for $n = 4$ and $n = 5$ means harder multiples, i.e. smaller separations.

Figure 3 shows the distribution of mass ratio, $q \equiv M_2/M_1$, against separation, a (strictly, semi-major axis). In all cases the mean mass ratio is high, viz. $\bar{q} = 0.74$, 0.83 and 0.65 for $n = 3$, 4 and 5, respectively. There is a tendency for closer binaries to have higher mass-ratios, i.e. more nearly equal components. This tendency arises because the formation of a close binary often entails hardening by ejection, and the ejections tend to remove the less massive objects; hence only the more massive objects are left as potential binary components, and the range

[1] Hubber & Whitworth (2005) have shown how the full range of binary parameters can be reproduced by considering a range of core parameters.

of possible masses is thereby reduced, pushing q towards unity. In addition, when a close binary accretes material with high angular momentum, the accreted material tends to end up on the less massive component, which again pushes q towards unity (Whitworth et al. 1995; Bate & Bonnell 1997; Papers I and II).

Such high mass ratios are not compatible with the observations, which, whilst they show a trend to more equal-mass companions in close binaries (e.g. Mazeh et al. 1992; White & Ghez 2001; Fisher et al. 2005), are certainly not as extreme as suggested by these results. However, a recent paper by Yasuhiro et al. (2005) suggests that accretion in a proto-binary system is generally onto the primary (especially in circular orbits) as angular momentum is removed from the accreting gas by spiral shocks. Such a mechanism is beyond the ability of these simulations to resolve and may help solve this problem.

4. Discussion

Delgardo Donate et al. (2004) have also explored the effect of the turbulent power spectrum on the fragmentation of low-mass cores, performing two ensembles of 5 SPH simulations each, one with $n = 3$ and one with $n = 5$. They use a slightly different core mass ($5.0\,M_\odot$, as compared with our $5.4\,M_\odot$), a different density profile (uniform, as compared with Eq. (1)), and a slightly different equation of state. However, the most significant difference is that their cores have a much higher initial level of turbulence; specifically, they adopt $\alpha_{\rm turb} = 1.0$, as compared with our $\alpha_{\rm turb} = 0.1$. As a consequence, the initial turbulent velocities in their cores are mildly supersonic and the cores are marginally unbound ($\alpha_{\rm turb} + \alpha_{\rm therm} \simeq 1.1$), whereas the initial turbulent velocities in our cores are subsonic and the cores are approximately virialised ($\alpha_{\rm turb} + \alpha_{\rm therm} \simeq 0.4$). The amount of turbulent energy has a profound influence on the outcome of collapse.

In the strongly turbulent cores of Delgado Donate et al. (2004), there is so much power in the turbulence that even the small-scale inhomogeneities created by small-scale turbulent motions can become self-gravitating and collapse (whereas in our simulations these small-scale inhomogeneities have much lower amplitude and tend to disperse). As a result, many more objects are formed, and – *in direct contrast with our results* – more objects are formed when $n = 3$ than when $n = 5$. This is because the same amount of power invested in small scales (large k) produces a larger number of inhomogeneities than when it is invested in large scales (small k). Furthermore, if more objects are formed in a core, then there have to be more ejections before a stable multiple is created, so the mass functions derived by Delgado Donate et al. (2004) have a larger tail of low-mass singles (low-mass stars and brown dwarfs), *and* this tail is larger when $n = 3$ than when $n = 5$.

With reference to Fig. 1, we suggest that the level of turbulence we have adopted is more representative of the cores in the Jijina et al. (1999) catalogue, and therefore probably more representative of the initial conditions in low-mass star forming cores, particularly if, as seems likely, some of the Jijina et al. cores are already collapsing, and therefore some of their nonthermal linewidth is attributable to collapse rather than initial turbulence. The low levels of turbulence we have invoked also seem to result in more acceptable values for the overall multiplicity.

5. Conclusions

We have investigated the influence of the slope of the turbulent power spectrum on the fragmentation of dense molecular cores, by means of an ensemble of SPH simulations. We consider a spherical, $5.4\,M_\odot$ core, with a Plummer-like density profile (Eq. (1)), and a low level of turbulence, $\alpha_{\rm turb} \equiv E_{\rm turb}/|\Omega| = 0.10$, similar to observed cores such as L1544. The turbulence has a power spectrum $P(k) \propto k^{-n}$ with $n = 3$, 4, or 5. The choice of n influences the number of objects that form, the mass function of those objects, and the properties of the multiple systems that they comprise. However, the process is chaotic, in the sense that even if n is fixed, different realizations of the turbulent velocity field can produce widely different stellar masses and binary properties. Our main conclusions are therefore statistical in nature, and could always be improved by performing more simulations:

- The average number of objects that form in a collapsing core increases monotonically with n, from $\bar{N}_{\rm obj} = 3.7 \pm 1.4$ when $n = 3$, to $\bar{N}_{\rm obj} = 5.5 \pm 3.0$ when $n = 5$.
- The mass function always involves a peak at $M \sim 1\,M_\odot$ and most of the objects in the peak are in multiple systems.
- As n increases and more objects are produced, more dynamical ejections are required before a stable multiple is formed, which has two consequences. (i) A larger proportion of single, low-mass objects (low-mass stars and brown dwarfs) is produced; hence the mass function develops a low-mass tail and the mean multiplicity decreases; (ii) the resulting binaries tend to be harder, i.e. to have smaller separations.
- The mean mass ratios of binary systems do not depend strongly on n, but close binaries tend to have mass ratios closer to unity, i.e. more nearly equal components. This is because the ejections which harden a binary preferentially remove low-mass objects, leaving the two most massive objects; the larger the initial number of objects, the more ejections are required, the harder the final binary, and the closer the masses of the two binary components.
- The low level of turbulence we have adopted in these simulations ($\alpha_{\rm turb} = 0.1$) appears to be in good agreement with observations of low-mass cores, and to reproduce the mean multiplicity in observed stellar populations.

These results do not match observed multiple systems very well. The separation distribution is too narrow and the mass ratios tend too much towards equal-masses. This is probably due in part to the fact that we consider only one (rather high) core mass. The separation distribution may well improve if a realistic range of core masses were considered (cf. Hubber & Whitworth 2005), but this would vastly increase the computational load as a far larger series of ensembles would be required. Even then, the small separation range is exacerbated by the hardening of systems through ejections when too many fragments are formed (see Goodwin & Kroupa 2005). The tendency to equal-mass binaries may be a result of unresolved physics in the inner accretion region (see Yasuhiro et al. 2005).

Acknowledgements. S.P.G. is a UKAFF Fellow. We thank B. Sathyaprakash and R. Balasubramanian for allowing us to perform these simulations on their Beowulf cluster. Part of this work was carried out while D.W.T. was on sabbatical at the Observatoire de Bordeaux, and he gratefully acknowledges the hospitality accorded to him there.

References

André, P., Ward-Thompson, D., & Barsony, M. 2000, in Protstars & Planets IV, ed. V. Mannings, A. P. Boss, & S. S. Russell (Tuscon: University of Arizona Press), 59

André, P., Ward-Thompson, D., & Motte, F. 1996, A&A, 314, 625

Barnes, J., & Hut, P. 1986, Nature, 324, 446

Bate, M. R., & Bonnell, I. A. 1997, MNRAS, 285, 33
Bate, M. R., Bonnell, I. A., & Price, N. M. 1995, MNRAS, 277, 362
Bate, M. R., Bonnell, I. A., & Bromm, V. 2002, MNRAS, 336, 705
Bate, M. R., Bonnell, I. A., & Bromm, V. 2003, MNRAS, 339, 577
Bonnell, I. A., Bate, M. R., Clarke, C. J., & Pringle, J. E. 2001, MNRAS, 323, 785
Bonnell, I. A., Bate, M. R., & Vine, S. G. 2003, MNRAS, 343, 413
Bonnell, I. A. 2003, private communication
Burkert, A., & Bodenheimer, P. 2000, ApJ, 543, 822
Delgardo-Donate, E. J., Clarke, C. J., & Bate, M. R. 2003, MNRAS, 342, 926
Delgardo-Donate, E. J., Clarke, C. J., & Bate, M. R. 2004, MNRAS, 347, 759
Duchêne, G. 1999, A&A, 341, 547
Duquennoy, A., & Mayor, M. 1991, A&A, 248, 485
Fisher, R. T. 2004, ApJ, 600, 769
Fisher, J., Schröder, K.-P., & Smith, R. C. 2005, MNRAS, 361, 495
Gawryszczak, A. J., Goodwin, S. P., Burkert, A., & Różyczka, M. 2006, A&A, submitted
Goodwin, S. P., & Kroupa, P. 2005, A&A, 439, 565
Goodwin, S. P., Whitworth, A. P., & Ward-Thompson, D. 2004a, A&A, 414, 633 (Paper I)
Goodwin, S. P., Whitworth, A. P., & Ward-Thompson, D. 2004b, A&A, 423, 169 (Paper II)
Hennebelle, P., Whitworth, A. P., Gladwin, P. P., & André, P. 2003, MNRAS, 340, 870
Hennebelle, P., Whitworth, A. P., Cha, S.-H., & Goodwin, S. P. 2004, MNRAS, 348, 687
Hubber, D. A., & Whitworth, A. P. 2005, A&A, 437, 113
Jijina, J., Myers, P. C., & Adams, F. C. 1999, ApJS, 125, 161
Kirk, J. M., Ward-Thompson, D., & André, P. 2005, MNRAS, 360, 1506
Larson, R. B. 1969, MNRAS, 145, 271
Masunaga, H., & Inutsuka, S. 2000, ApJ, 531, 350
Mathieu, R. D. 1994, ARA&A, 32, 465
Mazeh, T., Goldberg, D., Duquennoy, A., & Mayor, M. 1992, ApJ, 401, 265
Monaghan, J. J. 1992, ARA&A, 30, 543
Myers, P. C. 1983, ApJ, 270, 105
Myers, P. C., Ladd, E. F., & Fuller, G. A. 1991, ApJ, 372, L95
Patience, J., Ghez, A. M., Reid, I. N., & Matthews, K. 2002, AJ, 123, 1570
Reipurth, B., & Zinnecker, H. 1993, A&A, 278, 81
Reipurth, B., & Clarke, C. 2001, ApJ, 122, 432
Tafalla, M., Myers, P. C., Caselli, P., & Walmsley, C. M. 2004, A&A, 416, 191
Tohline, J. E. 1982, Fundamentals of Cosmic Physics, 8, 1
Ward-Thompson, D., Scott, P. F., Hills, R. E., & André, P. 1994, MNRAS, 268, 276
Ward-Thompson, D., Motte, F., & André, P. 1999, MNRAS, 305, 143
White, R. J., & Ghez, A. M. 2001, ApJ, 556, 265
Whitworth, A. P., Chapman, S. J., Bhattal, A. S., et al. 1995, MNRAS, 277, 727
Whitworth, A. P., & Ward-Thompson, D. 2001, ApJ, 547, 317
Yasuhiro, O., Sugimoto, K., & Hanawa, T. 2005, ApJ, 623, 922